

**Basic Drive Parameters of PACS FM Chopper
Specific Torque,
Open Loop Oscillation Frequency & Damping
from FM ILT tests
PCD req. 2.3.1**

U. Klaas¹, J. Schreiber¹, H. Dannerbauer¹

¹ Max-Planck-Institut für Astronomie,
Königstuhl 17, D-69117 Heidelberg, Germany

Req. 2.3.1 Angular Calibration of PACS FM Chopper - Open Loop Measurements

2.3.1 - A. History

Version	Date	Author(s)	Change description
1.0	November 24, 2006	U. Klaas (MPIA), J. Schreiber (MPIA), H. Dannerbauer (MPIA)	Drive parameters from 3 coils open loop operation with QM DECMEC

2.3.1 - B. Summary

Open loop measurements operating the chopper without the position control electronics were performed in order to characterise the static angle vs. current relation and thus derive the basic drive parameter of the specific torque. This can be compared with the module level characterisation performed at Carl Zeiss. The swing-in behaviour was recorded for the angular range $-9^\circ < \Phi < +9^\circ$.

The offset corrected angular calibration of field plate 1 as described in PICC-MA-TR-009 was applied. The correctness of this calibration is still under investigation at this moment!

The angle vs. drive current relation found during FM-ILT is different from the one established at Carl Zeiss. For the inner angle range only 90% and for the outer angle range only 80% of the drive current required at module level for the same angular deflection are needed.

Consequently the derived specific torque - assuming no change in the spring rate - is in absolute terms higher by 10 – 20% than at module level. Also in the Zeiss results the spring rate is just a constant multiplication factor which was derived from independent torque measurements of the flexural pivots.

The shape of the specific torque curve with angle differs significantly from the one established at module level at Carl Zeiss.

Inspecting the behaviour of the specific torque, the swing-in frequency and the swing-in damping rate with deflection angle significant discontinuities show up at angles around -5° and $+5^\circ$.

Together with the large offset of about 1 deg of the mechanical zero point between FM-ILT and Zeiss module level measurements (see RD2) the discontinuous behaviour of the drive characteristics causes a severe concern about a non-conformance of the chopper system after delivery by Zeiss. Affected components may be the flexural pivots, the air gaps and magnets of the drive, but also the current source of the control electronics. This should be urgently investigated and clarified by all applicable means, since it certainly has also significant impact on the dynamic behaviour of the chopper and on the longer term significant degradations may show up during the mission.

2.3.1 - C. Data Reference Sheet

Ref	Date	Archive filename
PACS Calibration Document req. 2.3.1	24-Mar-2006	PACS-MA-GS-001 (RD1)
Angular Calibration of PACS FM Chopper for FM ILT tests (PCD req. 2.3.1)	10-Nov-2006	PICC-MA-TR-009 (RD2)
Electrical Interface Control Document for PACS chopper FS (selected as actual flight model)	24-May-2006	PACS-MA-TN-778 (RD3) spring constant of flex pivots specific torque measurement damping constant, eigenfrequency as determined at Carl Zeiss
PACS Chopper Flight Spare Model User Manual and Handling Procedure	09-Jan-2006	PACS-MA-HM-755 (RD4) for calibration at Zeiss
DECMEC Housekeeping Data & Calibration	08-Aug-2006	PACS-CL-TN-041 V 2.1 (RD5) chapter 5.2 chopper output amplifier and housekeeping chapter 5.2.1: QM data
FM-ILT Chopper open loop measurement nominal mode (3 coils + QM DECMEC)	08-Nov-2006	FILT_Chopper_open_loop.03.tm
FM-ILT Chopper open loop measurement nominal mode (3 coils + QM DECMEC)	10-Nov-2006	FILT_Chopper_open_loop.05.tm

2.3.1 - D. Test Description

For a general overview on the subject and test design, see RD1.

2.3.1 - D.1. Specific Torque

RD3, chapter 2.1.1 provides the chopper transferfunction (without resonances):

$$\Phi = \frac{U_{in}}{a_0 + a_1 \cdot p + a_2 \cdot p^2 + a_3 \cdot p^3}$$

$$\begin{aligned} a_0 &= \frac{R \cdot c}{S} \\ a_1 &= \frac{R \cdot D + L \cdot c + S^2}{S} \\ a_2 &= \frac{L \cdot D + R \cdot J}{S} \\ a_3 &= \frac{L \cdot J}{S} \\ D &= 2 \cdot J \cdot d \end{aligned}$$

Φ :	deflection	[rad]
U_{in} :	input voltage	[V]
p :	complex frequency	$p = i \cdot \omega$
S :	specific torque	[N m A ⁻¹]
R :	coil resistance	[Ω]
c :	spring rate	[N m rad ⁻¹]
D :	damping constant	[kg m ² s ⁻¹]
d :	decay constant	[s ⁻¹]
J :	moment of inertia	[kg m ²]
L :	coil inductance	[H]

One notices that the specific torque S is an important parameter of the drive characterisation. Under static conditions, with $p = 0$

$$\begin{aligned} \Phi &= \frac{U_{in}}{a_0} = \frac{U_{in} \cdot S}{R \cdot c} \\ S &= \frac{R \cdot c \cdot \Phi}{U_{in}} = c \cdot \frac{\Phi}{I} \end{aligned}$$

i.e. the specific torque can be determined from static deflection measurements by applying a drive current I and measuring the resulting deflection Φ . The spring rate must be independently measured and is taken from RD3 as the total spring rate $c = 7.68 \text{ N mm rad}^{-1}$ for the springs of the two flexural pivots.

In practice the measurement was performed by commanding discrete drive currents in regular steps of $\approx 1 \text{ mA}$ in the range $\pm 15 \text{ mA}$. Each current level between the maximum drive currents was measured with a current step upwards and a current step downwards which allows to check for hysteresis effects. Fig. 1 shows the sequence recorded in TM-file `FILT.Chopper.open.loop_05.tm`.

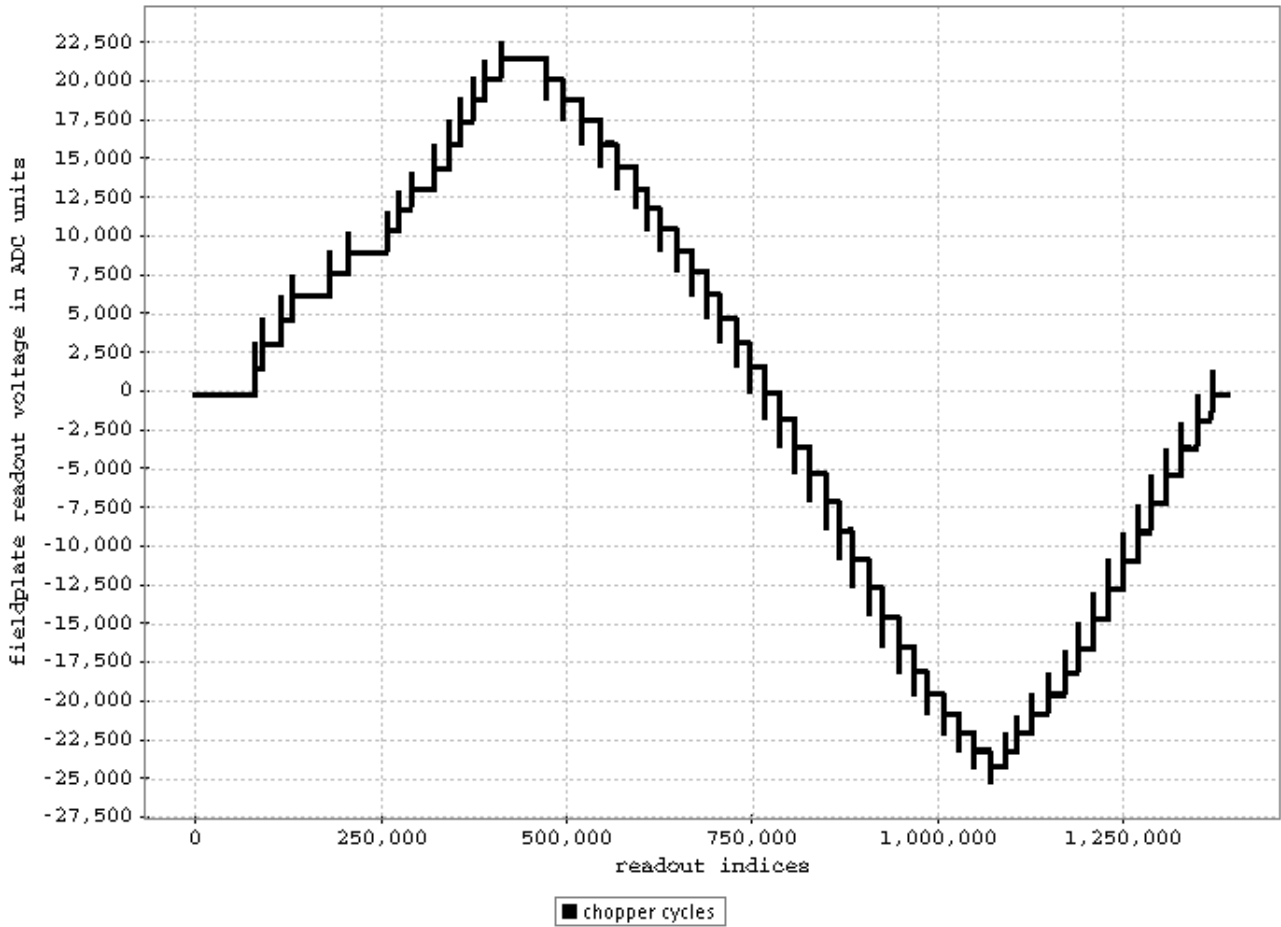


Figure 1: Measurement sequence of FILT.Chopper_open_loop_05.tm. Nominal commanded currents were 0, +1, +2, ..., +14, +15, +14, ..., +1, 0, -1, -2, ... -14, -15, -14, ..., -1, 0 mA, assuming a conversion for the commanding units $COU = \frac{I}{133 mA} \cdot 32767$. For the actual resulting currents see the Results section.

2.3.1 - D.2. Open loop plateau swing-in oscillation and damping

When applying the drive current under open loop conditions the chopper is deflected to the angle Φ , but shows a damped oscillation when swinging in into the new plateau

$$\Phi(t) = \Phi_0 + \Delta\Phi \cdot e^{-\delta \cdot t} \cdot \cos(\omega \cdot t)$$

Φ_0 :	final balanced plateau deflection	[rad]
$\Delta\Phi$:	max. amplitude of damped swing-in	[rad]
δ :	damping constant of swing-in oscillation	[s ⁻¹]
ω :	oscillation frequency	[Hz]

The damping constant can be determined by measuring the peak height at two different times t_1 and t_2 , i.e. $\cos(\omega \cdot t_1)$ and $\cos(\omega \cdot t_2) = 1$, and determining the ratio

$$\frac{\Phi(t_1)}{\Phi(t_2)} = \frac{e^{-\delta \cdot t_1}}{e^{-\delta \cdot t_2}}$$
$$\ln\left(\frac{\Phi(t_1)}{\Phi(t_2)}\right) = \delta \cdot (t_2 - t_1)$$
$$\delta = \frac{\ln\left(\frac{\Phi(t_1)}{\Phi(t_2)}\right)}{(t_2 - t_1)}$$

or technically as the slope of a fit to $\ln(\Phi_{\text{peak}}(t_i))$ over t . A minimum threshold for $\Phi(t_i)$ restricts the number of reliable peaks in the fit.

Alternatively the time constant τ

$$\tau = \frac{1}{\delta} \quad [s]$$

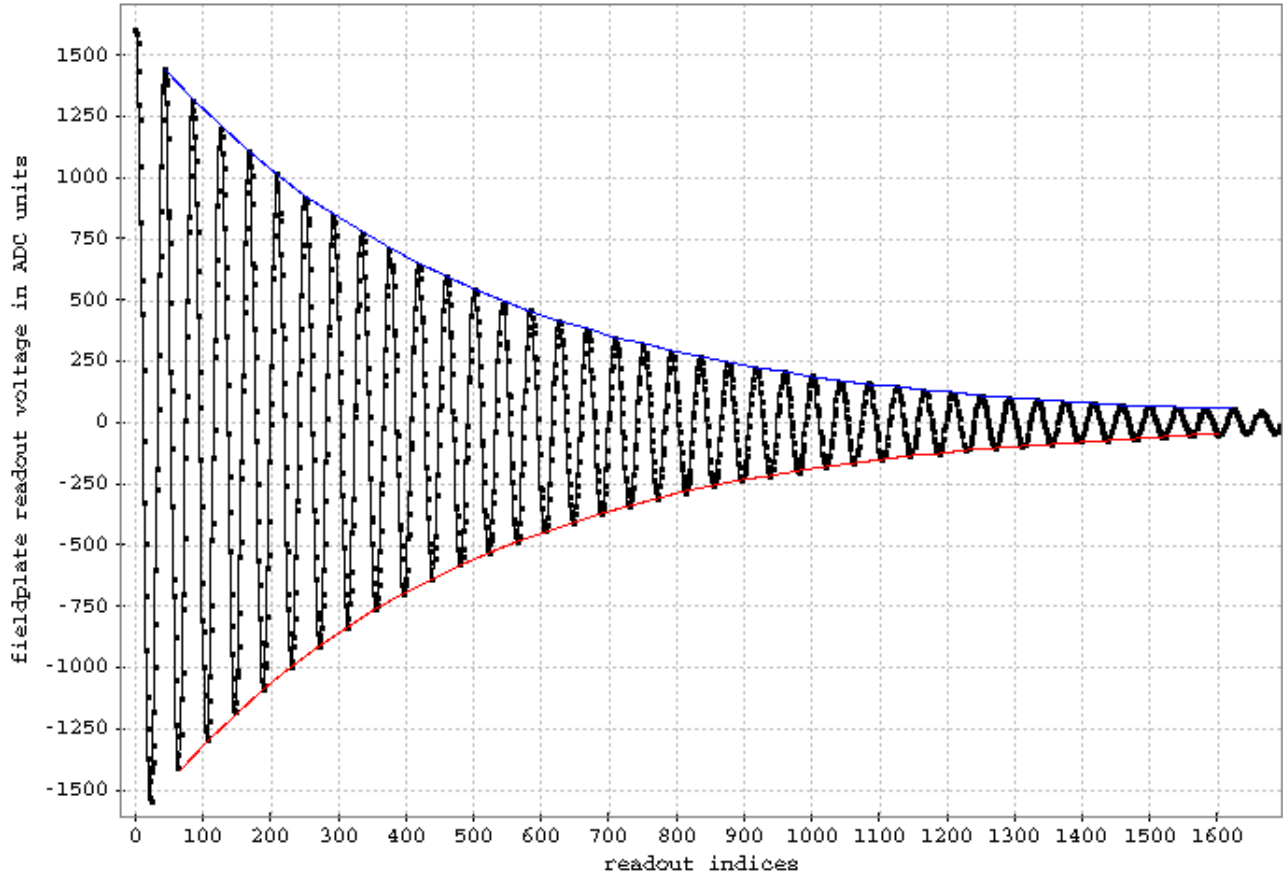
is specified.

Figs. 2 and 3 show two examples for damped oscillations of the sequence displayed in Fig. 1 occurring at two different elongations. While the oscillation in Fig. 2 behaves very well with a good fit result for δ , there is some modulation on top of the exponential decay for Fig. 3 resulting in a less good fit. A possible explanation for this different behaviour is given in the results section.

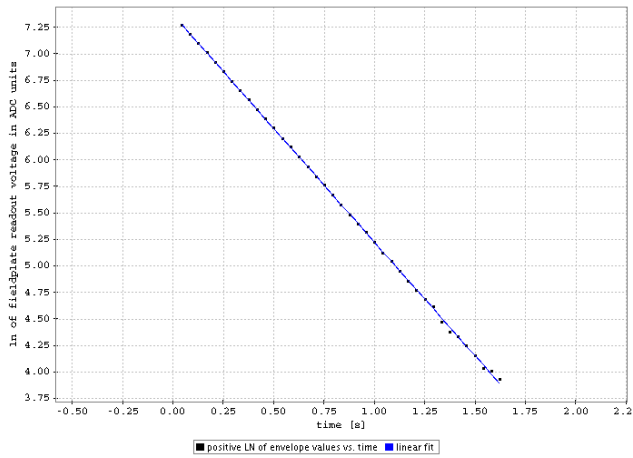
The oscillation frequency is determined as the average of the time differences between oscillation peaks

$$\omega = \frac{1}{n} \sum_{i=1}^n \frac{1}{\Delta t(\text{peak}_{i+1} - \text{peak}_i)}$$

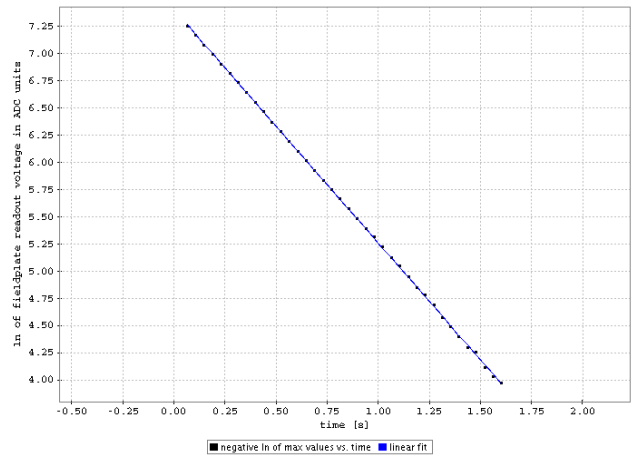
It should be noted that this method is different from the method Carl Zeiss used to determine the resonance frequency R_c and decay constant d in RD3. They deflected the chopper to a certain angle and then interrupted the current supply by a switch with the chopper system consequently freely swinging out around the zero position. In the tests performed here the load by the current source cannot be disconnected.



■ chopper open loop oscillation - fitted straight line offset ■ fitted positive model ■ fitted negative model



■ positive LN of envelope values vs. time ■ linear fit



■ negative ln of max values vs. time ■ linear fit

Figure 2: Damped swing-in of the chopper onto a plateau with an angular deflection of 0.5° coming from an elongation of 1.03° (DMC ROU = 1537, cf. Table 1). The damped oscillation shows a very well behaving exponential decay as can be seen from the fits to the ln of the positive and negative peak heights.

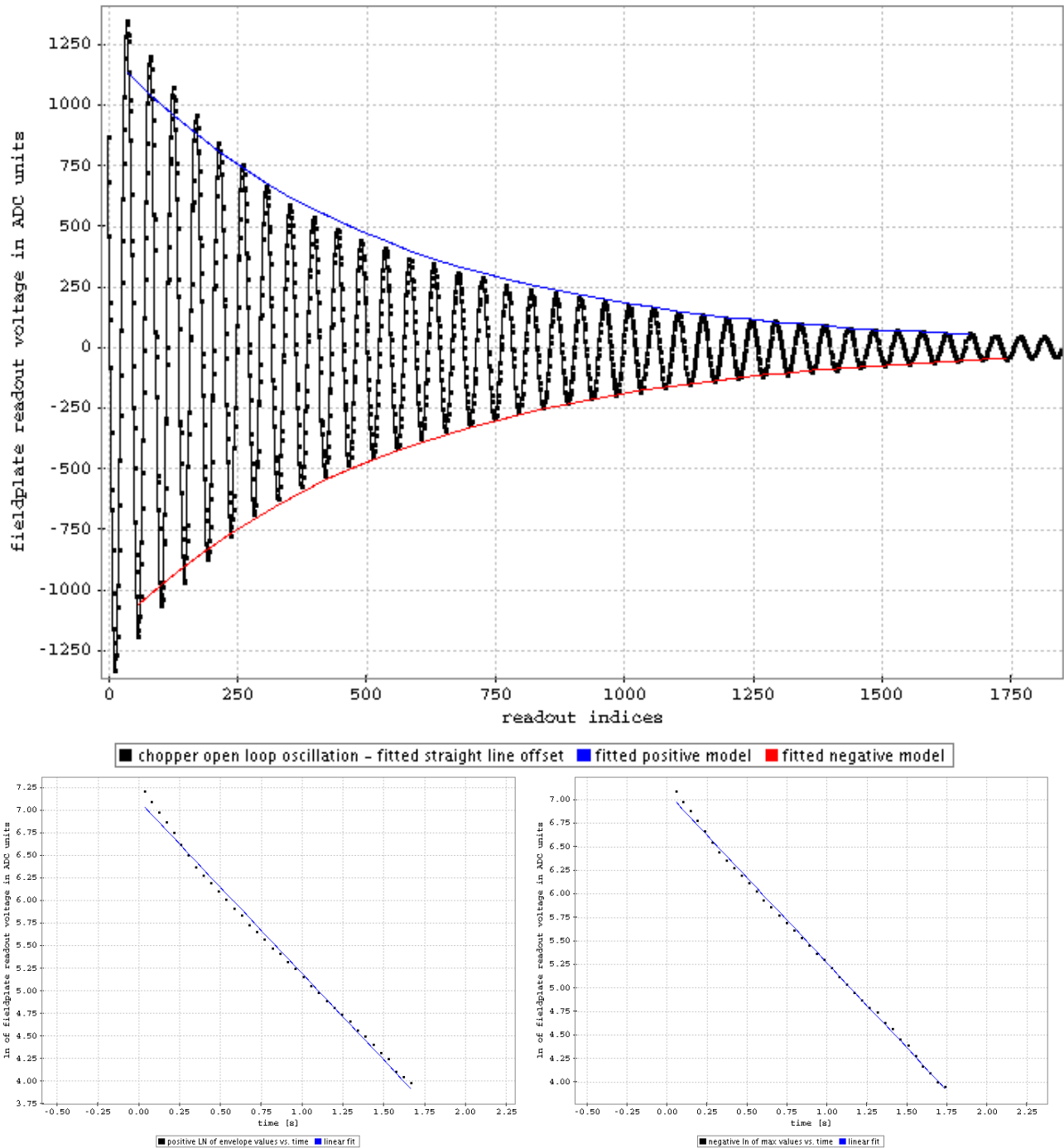


Figure 3: Damped swing-in of the chopper onto a plateau with an angular deflection of 5.117° coming from an elongation of 5.726° (DMC ROU = 14404, cf. Table 1). The damped oscillation does not follow a pure exponential decay, but there is another modulation on top as can be seen from the fits to the ln of the positive and negative peak heights.

2.3.1 - E. Results

2.3.1 - E.1. Angle vs. static current relation

Table 1 provides a compilation of the results from TM-File FILT_Chopper_open_loop_05.tm. The chopper angle is derived from the DECMEC read-out units applying the offset corrected angular calibration for the nominal field plate 1 as described in RD2. The chopper amplifier output current is contained in the diagnostic HK parameter DMC_CHOP_IA. The specific test was performed with 1 kHz HK and the parameter had not been specified as output. However, it is possible to derive the actual output current value from the command value COU_{target} according to the conversion described in RD5 and verify this calibration for test data FILT_Chopper_open_loop_03.tm (confined to ± 4 mA) for which parameter DMC_CHOP_IA is available, see Table 2. We used the conversion

$$\begin{aligned} \text{current} &= a + m \cdot COU_{target} \\ \text{with } a &= 0.155047 \text{ mA} \\ m &= -0.00397074 \text{ mA} / COU_{target} \end{aligned}$$

Note that for a commanded current of 0 mA actually a small current of 0.155 mA is applied.

Note that for a consistent description that positive deflections belong to positive currents and negative deflections belong to negative currents the current values of Tables 1 and 2 will be multiplied by -1.

For comparison in Table 3 the static angle versus current relation measured at Zeiss and documented in RD4 are given.

Fig. 4 shows the angle versus current relations for FM-ILT and derived during the module level tests at Carl Zeiss. For this comparison the Zeiss relation has been corrected for the angular offset of the mechanical zero point found for the module level tests ($\Phi_{mz_MLT} = -0.376^\circ$). There is a evident difference between the two relations. The drive current needed for a certain angular deflection is smaller under FM-ILT conditions than under module level test conditions.

In order to quantify this difference Fig. 5 shows the ratio of the drive currents for the angle range $-9^\circ < \Phi < +9^\circ$ after fitting both measured relations with 6th order polynomials. The drive current needed for a certain angular deflection under FM-ILT conditions amounts to only 80 – 90% of the current needed during module level tests. The 80% apply to larger angles, the 90% to smaller angles.

In Fig. 6 the reproducibility of the angle versus drive current relation is investigated. Although there are some slight differences between results from TM files FILT_Chopper_open_loop_03.tm and FILT_Chopper_open_loop_05.tm they are consistent among themselves within the range of the hysteresis effect (see next subsection) and differ from the relation found at Zeiss module level tests. It should be noted that TM file FILT_Chopper_open_loop_03.tm was recorded before the control loop optimisation tests while TM file FILT_Chopper_open_loop_05.tm was recorded after the control loop optimisation tests.

Table 1: Angle vs. static open loop current relation from TM-File FILT_Chopper_open_loop_05.tm. The sequence of measurements went down the table columns for the positive branch and up the table columns for the negative branch.

positive branch			negative branch		
current (mA)	deflection (readouts)	angle (degrees)	current (mA)	deflection (readouts)	angle (degrees)
0.155	-222	-0.071	0.1551	-228	-0.073
-0.822	1424	0.462	1.132	-1939	-0.620
-1.799	3023	1.000	2.109	-3695	-1.173
-2.779	4579	1.514	3.089	-5485	-1.731
-3.756	6080	2.032	4.066	-7290	-2.290
-4.737	7538	2.546	5.047	-9117	-2.854
-5.714	8947	3.054	6.024	-10946	-3.422
-6.695	10320	3.558	7.005	-12815	-4.003
-7.671	11648	4.053	7.891	-14771	-4.654
-8.648	13011	4.564	8.958	-16612	-5.285
-9.629	14357	5.099	9.939	-18192	-5.850
-10.606	15909	5.711	10.916	-19605	-6.380
-11.583	17393	6.314	11.893	-20903	-6.892
-12.563	18811	6.913	12.873	-22109	-7.393
-13.540	20143	7.504	13.850	-23228	-7.882
-14.521	21390	8.086	14.831	-24275	-8.365
-13.540	20156	7.510	13.850	-23216	-7.877
-12.563	18833	6.923	12.873	-22084	-7.382
-11.583	17544	6.376	11.893	-20866	-6.877
-10.606	15948	5.726	10.916	-19552	-6.359
-9.629	14404	5.117	9.939	-18124	-5.825
-8.648	13053	4.580	8.958	-16524	-5.254
-7.671	11768	4.098	7.981	-14647	-4.612
-6.694	10444	3.604	7.005	-12691	-3.962
-5.714	9073	3.100	6.024	-10826	-3.384
-4.737	7665	2.591	5.047	-8998	-2.818
-3.756	6207	2.076	4.066	-7173	-2.254
-2.779	4704	1.557	3.089	-5369	-1.695
-1.799	3144	1.030	2.109	-3582	-1.138
-0.822	1537	0.499	1.132	-1828	-0.584
0.1551	-122	-0.039			

Table 2: Angle vs. static open loop current relation from TM-File FILT_Chopper_open_loop_03.tm. The sequence of measurements went down the table columns for the positive branch and up the table columns for the negative branch.

positive branch			negative branch		
current (mA)	deflection (readouts)	angle (degrees)	current (mA)	deflection (readouts)	angle (degrees)
-0.821	1354	0.439246			
-1.801	2960	0.968982			
-2.780	4523	1.49530			
-3.760	6033	2.01534	4.064	-7281	-2.28738
-2.780	4537	1.50007	3.090	-5489	-1.73239
-1.801	2983	0.976646	2.110	-3713	-1.17845
-0.821	1379	0.447416	1.131	-1971	-0.629627

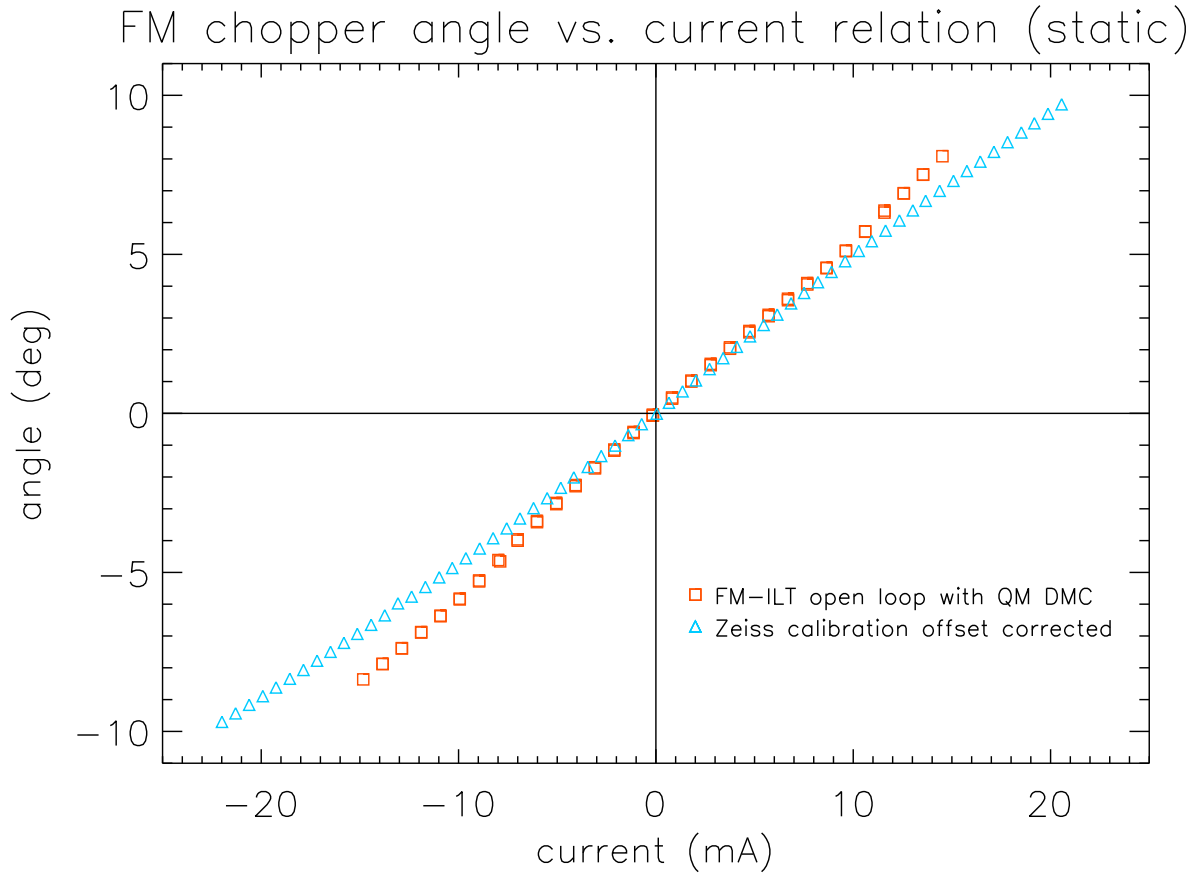


Figure 4: Resulting static chopper deflection angle when applying a drive current under open loop condition and after damping of the swing-in oscillation. For comparison the angle-current relation determined on module level at Carl Zeiss is shown. The Zeiss relation has been corrected for the angular offset of the mechanical zero point.

Table 3: Angle vs. static current relation measured during module level tests at Carl Zeiss at 4.2 K (RD4).

negative branch		positive branch	
current (mA)	angle (degrees)	current (mA)	angle (degrees)
-21.99	-10.0768		
-21.30	-9.8089		
-20.61	-9.5393	20.56	9.3421
-19.92	-9.2679	19.87	9.0446
-19.25	-8.9948	19.18	8.7450
-18.55	-8.7200	18.52	8.4561
-17.86	-8.4435	17.82	8.1527
-17.17	-8.1527	17.13	7.8475
-16.49	-7.8730	16.44	7.5404
-15.81	-7.5917	15.76	7.2444
-15.13	-7.3089	15.08	6.9339
-14.43	-7.0247	14.38	6.6218
-13.74	-6.7260	13.67	6.3080
-13.07	-6.3490	13.02	6.0059
-12.38	-6.1374	12.34	5.6892
-11.68	-5.8345	11.64	5.3711
-10.98	-5.5303	10.94	5.0383
-10.32	-5.2381	10.28	4.7309
-9.63	-4.9315	9.59	4.4090
-8.93	-4.6237	8.90	4.0725
-8.25	-4.3014	8.21	3.7484
-7.56	-3.9916	7.51	3.4097
-6.89	-3.6807	6.85	3.0837
-6.20	-3.3555	6.15	2.7297
-5.51	-3.0429	5.46	2.4021
-4.82	-2.7160	4.77	2.0465
-4.16	-2.3884	4.10	1.7177
-3.45	-2.0602	3.41	1.3611
-2.77	-1.7177	2.72	1.0177
-2.07	-1.3885	2.03	0.6603
-1.40	-1.0589	1.35	0.3164
-0.72	-0.7153	0.66	-0.0413
0.04	-0.3852		

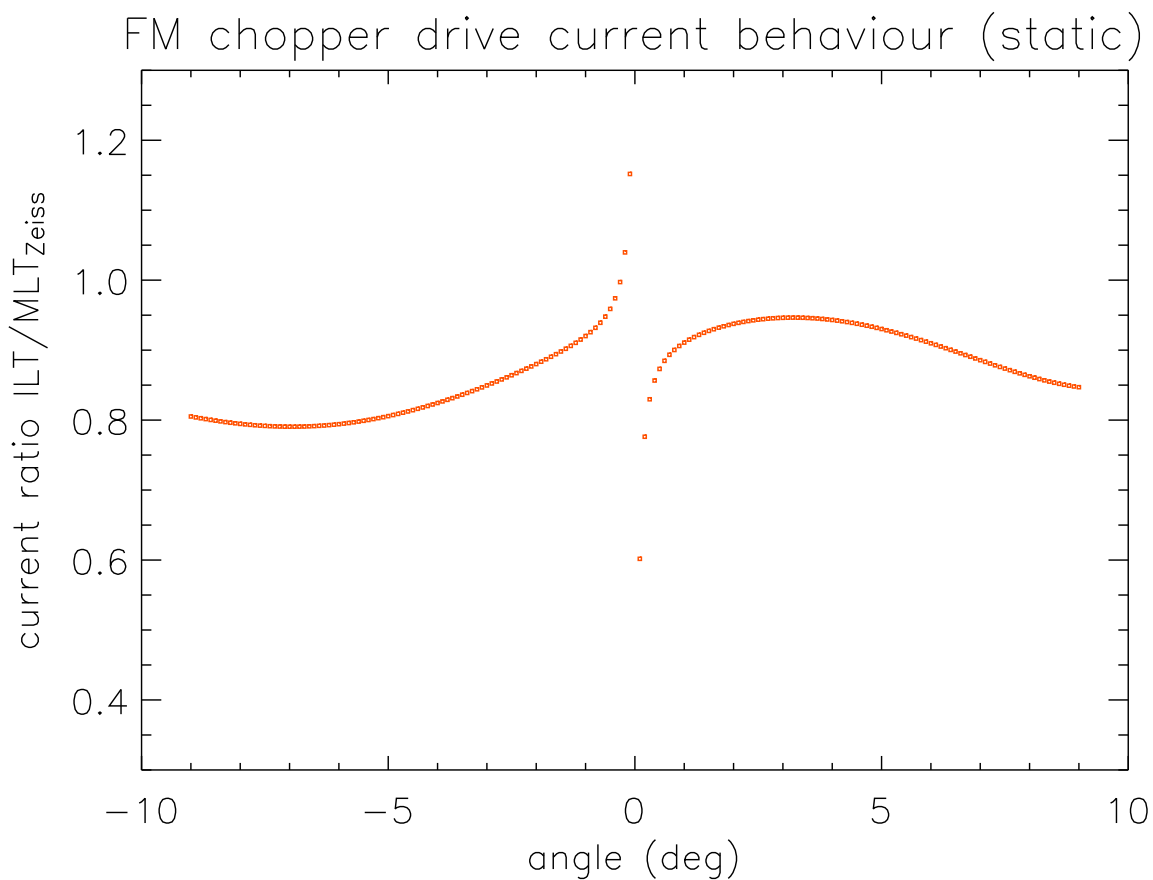


Figure 5: Ratio of chopper drive currents between FM-ILT configuration (chopper integrated in FPU) and module level tests (MLT) at Zeiss for the angle range $-9^\circ < \Phi < +9^\circ$. The discontinuity at $\Phi = 0^\circ$ is caused by non-perfect offset correction and accuracy limits in measuring small currents.

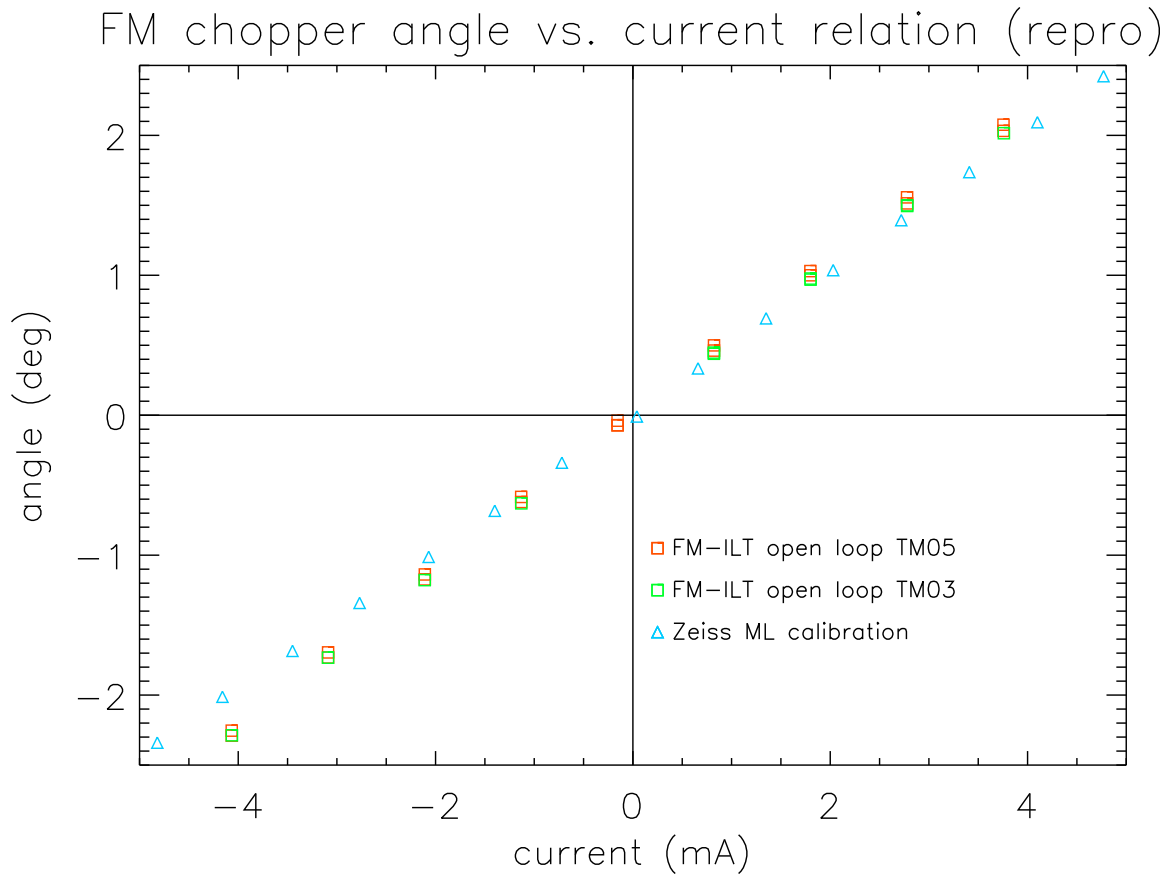


Figure 6: Reproducibility of the chopper deflection angle versus drive current relation for angles in the range $-2.5^\circ < \Phi < +2.5^\circ$ by comparing the results of TM file FILT_Chopper_open_loop_03.tm (taken before control loop optimisation tests) and TM file FILT_Chopper_open_loop_05.tm (taken after control loop optimisation tests). For comparison again the angle-current relation determined on module level at Carl Zeiss is shown. The Zeiss relation has been corrected for the angular offset of the mechanical zero point.

2.3.1 - E.2. Specific Torque

Fig. 7 is a direct translation of Fig. 4, since the torque T

$$T = \Phi[\text{rad}] \cdot c$$

is just a scaling of the angle converted to radian with the constant spring rate $c = 7.68 \text{ N mm rad}^{-1}$ of the flexural pivots as measured by Carl Zeiss.

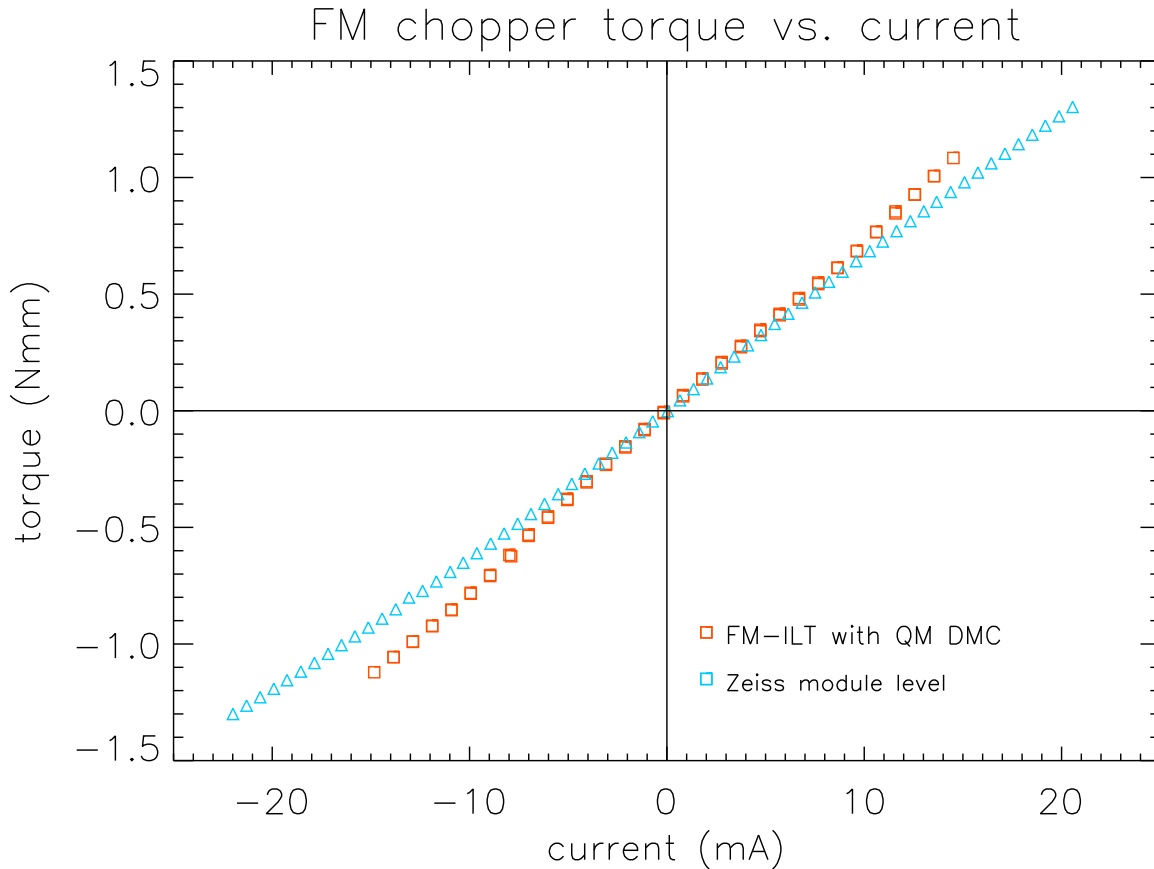


Figure 7: Torque vs. current relation both for the module level tests at Carl Zeiss and the FM-ILT open loop tests. This figure is directly related to Fig. 2, since the torque is the product of the angle (in rad) with the spring rate of the flexural pivots. The latter one is assumed to be constant with angle and to have a unique value of $7.68 \text{ N mm rad}^{-1}$ as measured by Carl Zeiss.

Fig. 8 shows the behaviour of the specific torque $\frac{T}{I}$ with angle both for the module level tests and the FM-ILT tests. We note several significant differences:

- The specific torque is higher during FM-ILT than during module level tests. This is a consequence of the smaller current needed in order to achieve a certain elongation.
- The asymmetry behaviour is different.
- We note turn-overs of the FM-ILT specific torque curve at around $\pm 5^\circ$.

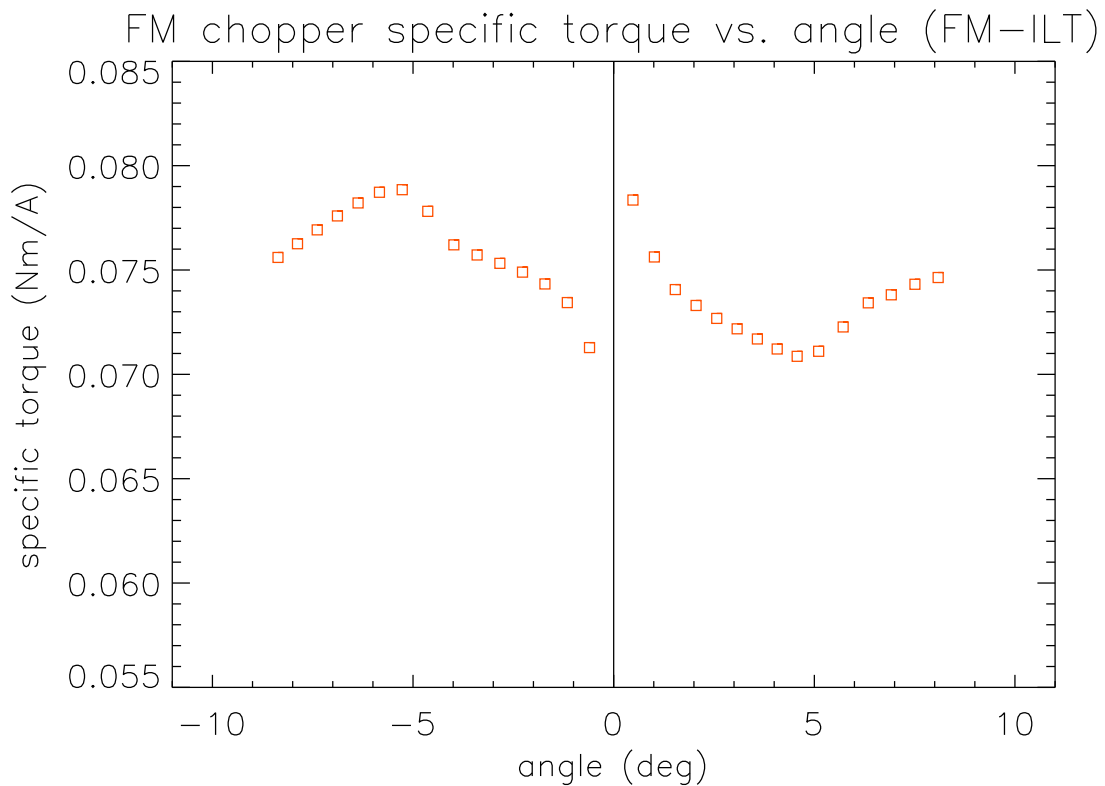
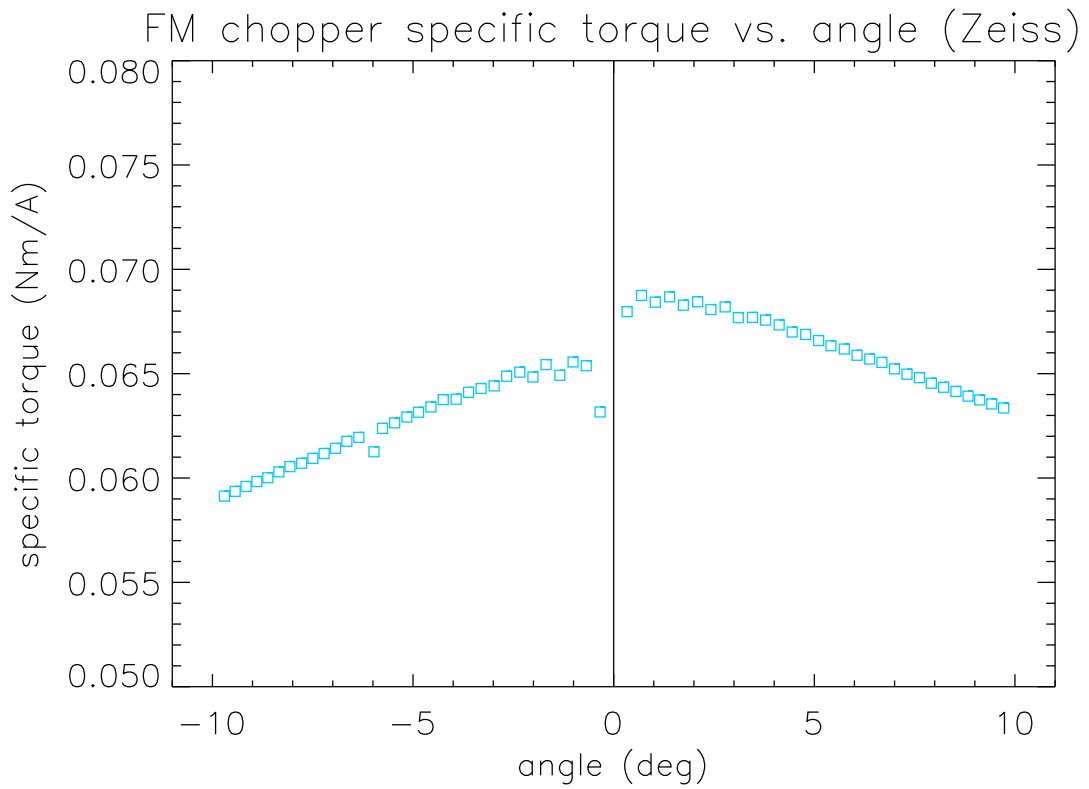


Figure 8: Specific torque of the chopper drive as measured on module level at Carl Zeiss (upper panel, cf. RD3, section 3.4.3) and during FM-ILT (lower panel).

2.3.1 - E.3. Plateau swing-in frequency and damping

Table 4 compiles the swing-in characteristics of the chopper for the open-loop measurement `FILT_Chopper_open_loop_05.tm`. Table 5 compiles the equivalent data for the open loop measurement `FILT_Chopper_open_loop_03.tm`. Since the latter one was only recorded with 256 Hz sampling and not with 1 kHz as the former one, the determination of the swing-in oscillation frequency is less accurate. Table 6 finally compiles the average swing-in frequencies and damping rates for each discrete angle measured during the sequence 05.

Fig. 9 shows the dependence of the frequency and damping rate with angle. No comparable measurement was performed on module level at Carl Zeiss. However we note for reference that from the swing-out measurements at Zeiss at LHe temperatures a resonance frequency of 24.8 ± 0.04 Hz and a damping rate of $\delta = 0.58 \pm 0.05 \text{ s}^{-1}$ (corresponding to $\tau = 1.724$ s) was determined. In Fig. 9 we note the clear discontinuities in the frequencies at angles around -5° and $+5^\circ$ and in the damping rate at the angle around $+5^\circ$. It is striking that the discontinuities and turn-overs of the specific torque curve occur at around the same angles. Also the extra modulations on top of the exponential decay of the swing-in oscillation as shown in Fig. 3 and flagged in Table 4 (footnote a) occur at these angles.

Table 4: Results of the evaluation of the swing-in oscillations of the open loop sequence recorded in TM-File FILT_Chopper_open_loop_05.tm and displayed in Fig. 1. Data were recorded with 1 kHz sampling.

index	ROU _{FP}	ω_{pos} (Hz)	$\Delta\omega_{\text{pos}}$ (Hz)	ω_{neg} (Hz)	$\Delta\omega_{\text{neg}}$ (Hz)	τ_{pos} (s)	$\Delta\tau_{\text{pos}}$ (s)	τ_{neg} (s)	$\Delta\tau_{\text{neg}}$ (s)
79050:82000	1424	24.033	0.591	23.991	0.535	0.500	0.038	0.484	0.038
91250:94500	3023	24.160	0.672	24.163	0.404	0.502	0.039	0.471	0.037
116000:119000	4579	24.296	0.456	24.336	0.494	0.480	0.038	0.483	0.039
130100:133000	6080	24.476	0.649	24.435	0.475	0.466	0.039	0.454	0.040
180050:182500	7538	24.580	0.735	24.580	0.584	0.455	0.039	0.453	0.038
206050:208500	8947	24.673	0.481	24.691	0.533	0.446	0.049	0.440	0.048
258100:260300	10320	24.775	0.489	24.775	0.426	0.440	0.051	0.435	0.049
274150:276300	11648	24.864	0.440	24.864	0.464	0.439	0.053	0.440	0.053
291200:293000	13011	24.955	0.563	24.978	0.649	0.435	0.063	0.435	0.063
321100:324000 ^a	14357	21.411	0.546	21.329	0.807	0.522	0.060	0.571	0.067
341100:344000	15909	21.277	0.365	21.265	0.460	0.557	0.056	0.554	0.056
357100:360000	17393	21.469	0.484	21.457	0.350	0.562	0.058	0.560	0.057
373400:376500 ^d	18811	21.561	0.360	21.583	0.406	0.573	0.090	0.552	0.093
389100:392000	20143	21.691	0.521	21.715	0.418	0.586	0.061	0.576	0.059
411100:414000	21390	21.827	0.566	21.827	0.567	0.583	0.063	0.568	0.060
473100:476000	20156	21.727	0.421	21.739	0.415	0.573	0.058	0.571	0.058
496200:499000	18833	21.603	0.396	21.574	0.495	0.580	0.062	0.571	0.062
520100:523000	17544	21.457	0.439	21.457	0.408	0.561	0.057	0.565	0.058
544400:547000	15948	21.265	0.309	21.277	0.449	0.583	0.062	0.574	0.060
568370:571000 ^a	14404	21.420	0.646	21.378	0.567	0.523	0.057	0.553	0.060
592200:595000	13053	24.947	0.505	24.914	0.620	0.490	0.057	0.487	0.054
609200:612000	11768	24.872	0.658	24.872	0.394	0.463	0.053	0.448	0.050
627150:629500	10444	24.793	0.361	24.735	0.603	0.463	0.049	0.455	0.049
647400:650000	9073	24.683	0.623	24.648	0.472	0.463	0.051	0.457	0.049
669200:671500	7665	24.557	0.400	23.891	2.131	0.467	0.049	0.459	0.049
688200:690500	6207	24.458	0.449	24.478	0.497	0.458	0.049	0.455	0.051
707200:709500	4704	24.356	0.478	24.338	0.491	0.456	0.049	0.450	0.049
728400:730500 ^c	3144	24.183	0.424	24.194	0.749	0.460	0.045	0.455	0.046
746400:749000 ^c	1537	24.066	0.377	24.057	0.378	0.466	0.044	0.466	0.046
767200:770000	-122	23.868	0.431	23.869	0.541	0.487	0.046	0.483	0.047
787200:790000 ^d	-1828	23.720	0.339	23.750	0.372	0.484	0.134	0.485	0.134
807200:810000	-3582	23.600	0.515	23.622	0.665	0.501	0.047	0.497	0.048
827300:830000	-5369	23.537	0.435	23.522	0.502	0.495	0.051	0.502	0.052
849300:852000	-7173	23.471	0.536	23.500	0.510	0.503	0.051	0.503	0.050
868200:871000 ^d	-8998	23.406	2.105	23.423	0.496	0.499	0.046	0.493	0.046
886250:889000	-10826	23.201	0.452	23.185	0.374	0.505	0.048	0.499	0.049
907300:910000	-12691	22.658	0.518	22.595	0.528	0.502	0.050	0.487	0.051
926200:929000 ^b	-14647	21.618	0.411	21.609	0.265	0.477	0.047	0.495	0.049
948250:950500 ^d	-16524	22.678	0.361	22.657	0.361	0.469	0.103	0.507	0.112
967500:970500	-18124	23.588	0.355	23.627	0.453	0.495	0.049	0.506	0.053
986300:989000 ^d	-19552	24.086	0.454	24.106	0.429	0.490	0.073	0.510	0.080
1009300:1012000	-20866	24.412	0.468	24.431	0.534	0.488	0.056	0.514	0.059
1027300:1030000	-22084	24.691	0.642	24.691	0.628	0.499	0.057	0.519	0.061
1048500:1051500	-23216	24.914	0.554	24.914	0.612	0.495	0.056	0.523	0.062
1070300:1073000	-24275	25.108	0.740	25.105	0.677	0.502	0.061	0.519	0.062

^a bad fit, modulation

^b slight modulation

^c good / very good fit

^d timing interference

Table 4: continued.

index	ROU _{FP}	ω_{pos} (Hz)	$\Delta \omega_{\text{pos}}$ (Hz)	ω_{neg} (Hz)	$\Delta \omega_{\text{neg}}$ (Hz)	τ_{pos} (s)	$\Delta \tau_{\text{pos}}$ (s)	τ_{neg} (s)	$\Delta \tau_{\text{neg}}$ (s)
1091300:1094000	-23228	24.893	0.560	24.914	0.495	0.500	0.060	0.522	0.062
1107500:1110000	-22109	24.674	0.602	24.683	0.582	0.500	0.057	0.512	0.057
1127300:1130000	-20903	24.457	0.639	24.455	0.561	0.495	0.055	0.510	0.056
1148300:1151000	-19605	24.096	0.535	24.127	0.610	0.494	0.054	0.519	0.055
1172500:1175000	-18192	23.632	0.526	23.632	0.441	0.497	0.050	0.506	0.051
1188300:1191000	-16612	22.783	0.460	22.755	0.452	0.496	0.049	0.511	0.050
1210300:1212500 ^b	-14771	21.622	0.442	21.574	0.385	0.484	0.046	0.502	0.048
1229300:1232500	-12815	22.478	0.544	22.479	0.470	0.501	0.046	0.486	0.047
1249300:1252000	-10946	23.145	0.575	23.114	0.512	0.499	0.047	0.499	0.049
1269400:1272000	-9117	23.388	0.490	23.385	0.617	0.499	0.051	0.496	0.049
1287550:1290000	-7290	23.471	0.400	23.500	0.513	0.498	0.049	0.496	0.049
1307400:1311000	-5485	23.559	0.548	23.537	0.387	0.503	0.050	0.492	0.050
1327400:1330000	-3695	23.617	0.572	23.632	0.525	0.497	0.049	0.500	0.050
1349400:1352000	-1939	23.688	0.482	23.718	0.505	0.497	0.052	0.498	0.052
1369400:1372000	-228	23.840	0.440	23.869	0.473	0.492	0.051	0.493	0.049

- ^a bad fit, modulation
- ^b slight modulation
- ^c good / very good fit
- ^d timing interference

Table 5: Results of the evaluation of the swing-in oscillations of the open loop sequence recorded in TM-File FILT_Chopper_open_loop_03.tm. Data were recorded with 256 Hz sampling.

index	ROU _{FP}	ω_{pos} (Hz)	$\Delta \omega_{\text{pos}}$ (Hz)	ω_{neg} (Hz)	$\Delta \omega_{\text{neg}}$ (Hz)	τ_{pos} (s)	$\Delta \tau_{\text{pos}}$ (s)	τ_{neg} (s)	$\Delta \tau_{\text{neg}}$ (s)
6700:7500	1350	23.986	1.102	23.970	1.174	0.511	0.033	0.505	0.035
17450:18200	2962	24.160	1.153	23.623	2.268	0.513	0.034	0.503	0.036
26950:27700	4521	23.317	2.632	24.285	1.172	0.508	0.038	0.503	0.037
44070:44800	6037	24.381	1.175	24.452	1.297	0.506	0.034	0.498	0.035
55340:56200	4538	23.836	2.189	24.268	1.170	0.499	0.034	0.502	0.034
62310:63200	2979	24.204	1.161	23.660	2.116	0.510	0.034	0.496	0.034
69180:69900	1383	23.986	1.102	23.970	1.097	0.518	0.035	0.507	0.035
74350:75000	-271	23.431	1.974	23.873	1.138	0.523	0.034	0.486	0.035
80190:81000	-1969	23.768	1.079	23.732	0.963	0.488	0.034	0.495	0.036
85580:86300	-3711	22.714	2.479	23.639	0.987	0.500	0.036	0.490	0.035
90160:90900	-5494	23.616	0.862	23.197	1.867	0.498	0.033	0.531	0.034
94780:95500	-7286	23.585	0.937	23.151	1.960	0.497	0.035	0.513	0.034
98880:99600	-286	23.840	1.031	23.868	1.047	0.500	0.023	0.483	0.023

Table 6: Average parameters of swing-in oscillation frequency and damping for discrete deflection angles of open loop sequence FILT_Chopper_open_loop_05.tm.

Φ (deg)	ω_{mean} (Hz)	$\Delta \omega_{\text{mean}}$ (Hz)	τ_{mean} (s)	$\Delta \tau_{\text{mean}}$ (s)
0.48063	24.03675	0.23512	0.479	0.02075
1.01016	24.175	0.28112	0.472	0.02087
1.53565	24.3315	0.23987	0.46725	0.02188
2.05382	24.46175	0.25875	0.45825	0.02238
2.56853	24.402	0.48125	0.4585	0.02188
3.0768	24.67375	0.26362	0.4515	0.02462
3.55589	24.7695	0.23487	0.44825	0.02475
4.07273	24.868	0.2445	0.4475	0.02613
4.58479	24.9485	0.29212	0.46175	0.02962
5.10806	21.3845	0.32075	0.54225	0.0305
5.71857	21.271	0.19787	0.567	0.02925
6.34494	21.46	0.21012	0.562	0.02875
6.91807	21.58025	0.20712	0.569	0.03837
7.50693	21.718	0.22187	0.5765	0.0295
8.08616	21.827	0.40058	0.5755	0.04349
-0.05634	23.8615	0.23562	0.48875	0.02412
-0.60194	23.719	0.21225	0.491	0.0465
-1.15521	23.61775	0.28462	0.49875	0.02425
-1.71324	23.53875	0.234	0.498	0.02538
-2.2721	23.4855	0.24487	0.5	0.02488
-2.83588	23.4005	0.4635	0.49675	0.024
-3.40294	23.16125	0.23912	0.5005	0.02412
-3.9922	22.5525	0.2575	0.494	0.02425
-4.63488	21.60575	0.18787	0.4895	0.02375
-5.26971	22.71825	0.20425	0.49575	0.03925
-5.83754	23.61975	0.22188	0.501	0.02538
-6.36957	24.10375	0.2535	0.50325	0.03275
-6.88415	24.43875	0.27525	0.50175	0.02825
-7.38731	24.68475	0.30675	0.5075	0.029
-7.87967	24.90875	0.27762	0.51	0.03
-8.36466	25.1065	0.50099	0.5105	0.04349

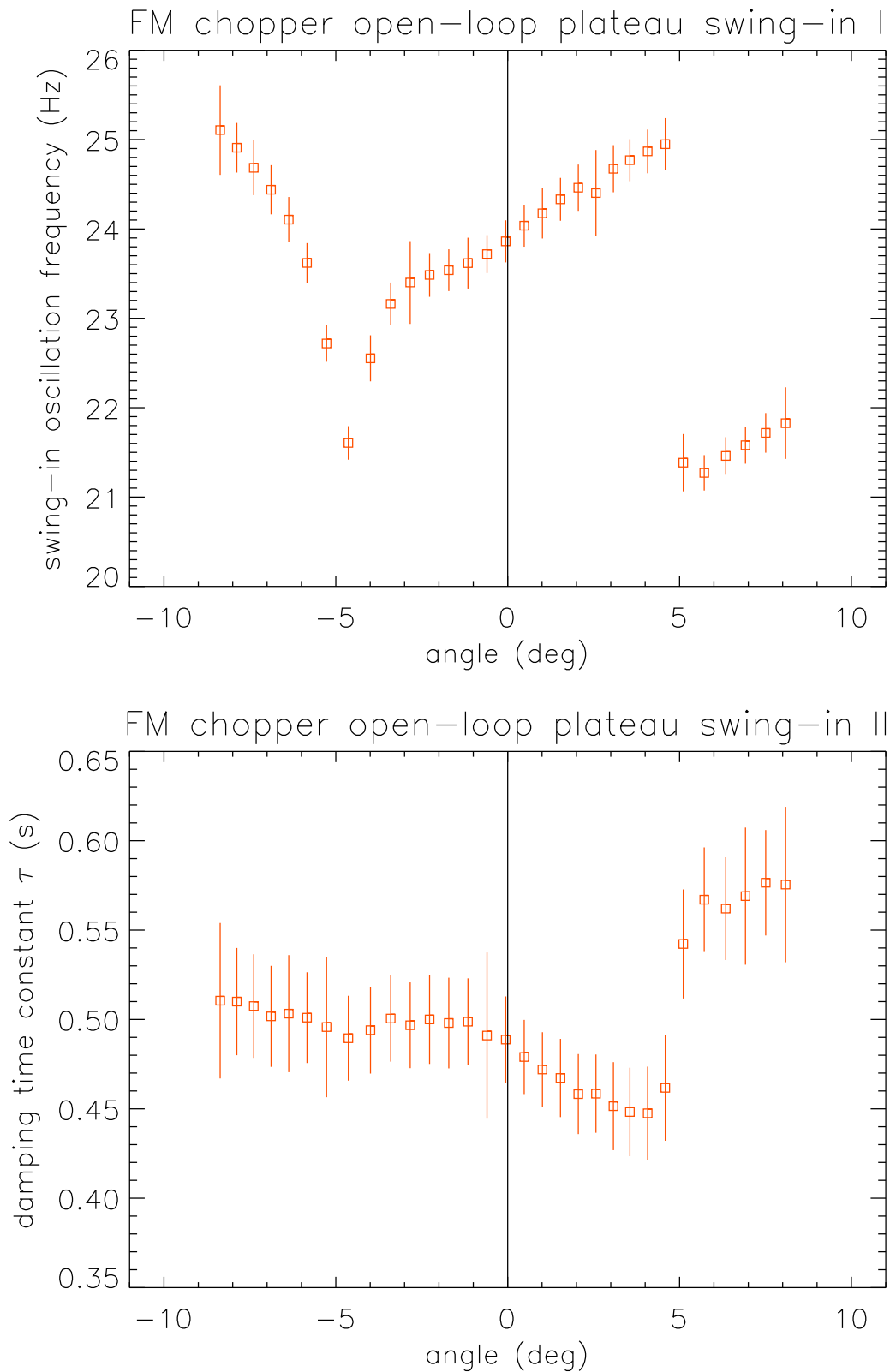


Figure 9: Variation of the swing-in oscillation frequency and damping time constant with angle for the open loop measurement FILT_Chopper_open_loop_05.tm. Input data are from Table 6.

2.3.1 - F. Conclusions

- The static angle vs. current relation of the chopper has been established from open loop measurements during FM-ILT for the angle range $-9^\circ < \Phi < +9^\circ$ and can be verified against the module level results. The angular calibration is based on the FM-ILT calibration of field plate 1. The current calibration is based on the DMC calibration for the chopper amplifier current.
- The angle vs. current relation during FM-ILT is significantly different from the one during module level tests. Reproducibility of this behaviour could be checked for currents in the range ± 4 mA.
- A smaller current is required in FM-ILT configuration than at module level in order to achieve the same angular deflection. It is $\approx 90\%$ in the inner and $\approx 80\%$ in the outer angle range.
- Assuming the same spring rate as for module level tests as a constant scaling factor the specific torque is derived from the angle vs. current relation and can be compared with the module level results. In absolute terms the specific torque is higher by 10 – 20% in FM-ILT than at module level. While this provides a more efficient drive there is concern about the shape of the specific torque curve with angle which shows discontinuities and turn-over points at about -5° and $+5^\circ$ which is not observed for the module level results.
- The swing-in behaviour for the angular $-9^\circ < \Phi < +9^\circ$ was evaluated from the damped oscillations by fitting exponential decay envelopes measuring the time difference between oscillation peaks. For this type of measurement the current source could not be disconnected in order to have only the freely swinging chopper system. Nevertheless resulting frequencies and damping rates are close to the resonance frequency and damping rate determined at module level.
- There is a variation of swing-in frequency and damping rate with angle. Again discontinuities are found at -5° and in particular at $+5^\circ$. The determination of the damping rate at this angle is more difficult because of a superimposed modulation.
- The systematic difference of the drive properties from module level results and the consistent occurrence of the discontinuities at the angles -5° and $+5^\circ$ not observed at module level cause severe concern about a non-conformance of the chopper system after delivery by Zeiss. This is reinforced by the unusually high offset of the mechanical zero point with regard to the one at module level.
- We recommend an investigation of possible reasons by the hardware teams. Affected components may be the flexural pivots, the air gaps and magnets of the drive, but also the current source of the control electronics.